



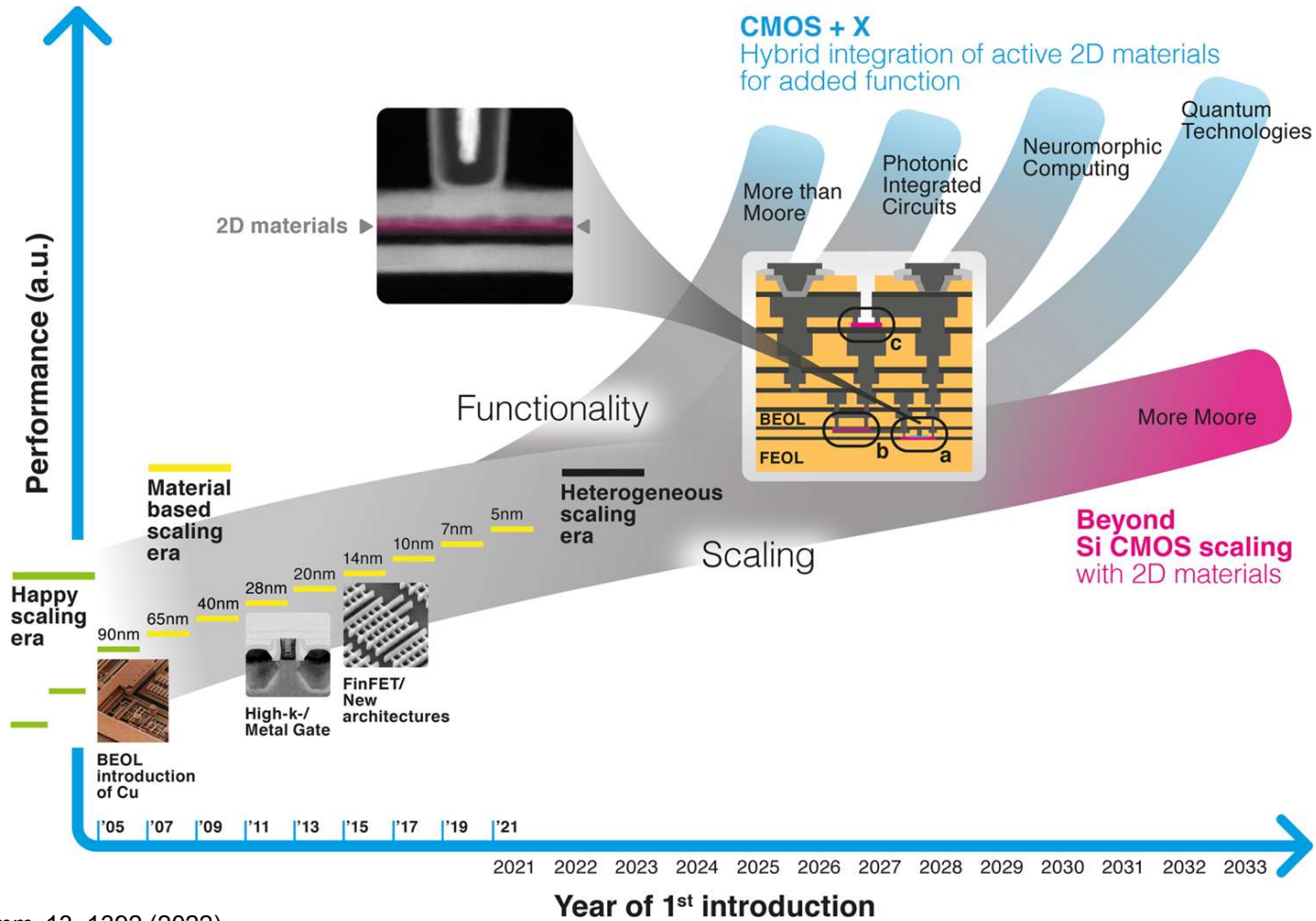
# Photoelectron spectroscopy in device technology: from XPS to HAXPES

O. Renault, P.-M. Deleuze, N. Gauthier and E. Martinez  
Univ. Grenoble-Alpes, CEA, Leti, 38054 Grenoble, France

FCMN Meeting | June 22nd, 2022

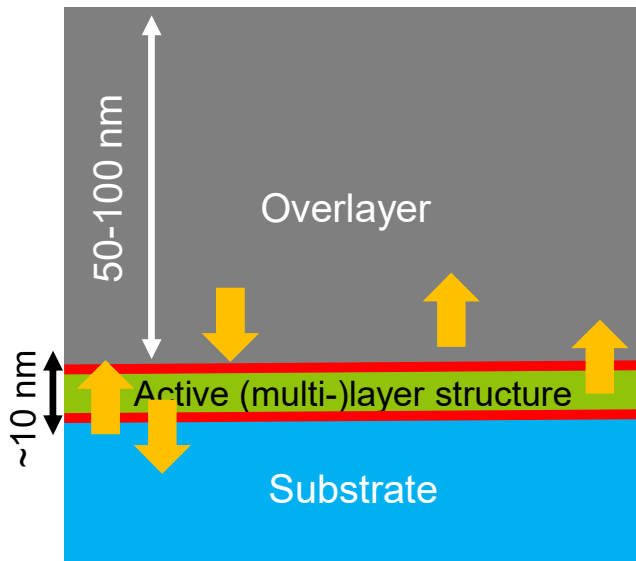


# Device technology context: new materials, critical interfaces

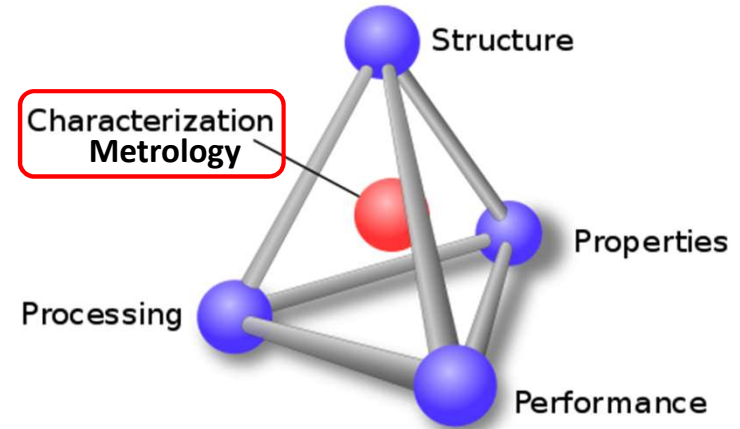
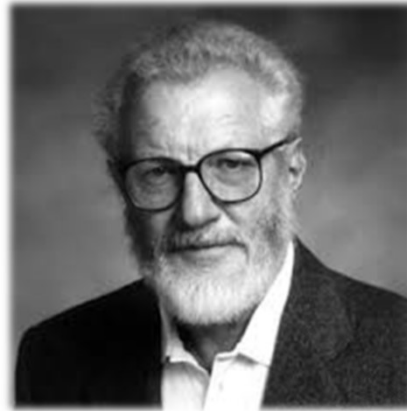


# Device technology context: new materials, critical interfaces

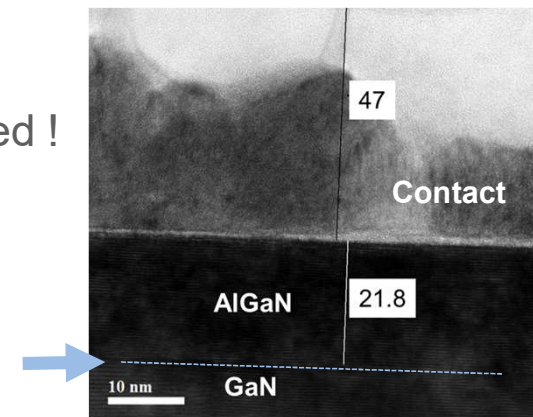
- « The interface is the device » ...  
*Herbert Kroemer, Nobel Lecture, dec. 8<sup>th</sup>, 2000*



— Critical interfaces  
→ Inter-diffusion



- ... but the interface is *deeply* buried !



# XPS for interfaces

- Advantages of XPS:

- Non-destructive
- In-line/fab-compatible
- Chemical fingerprinting
- Quantification

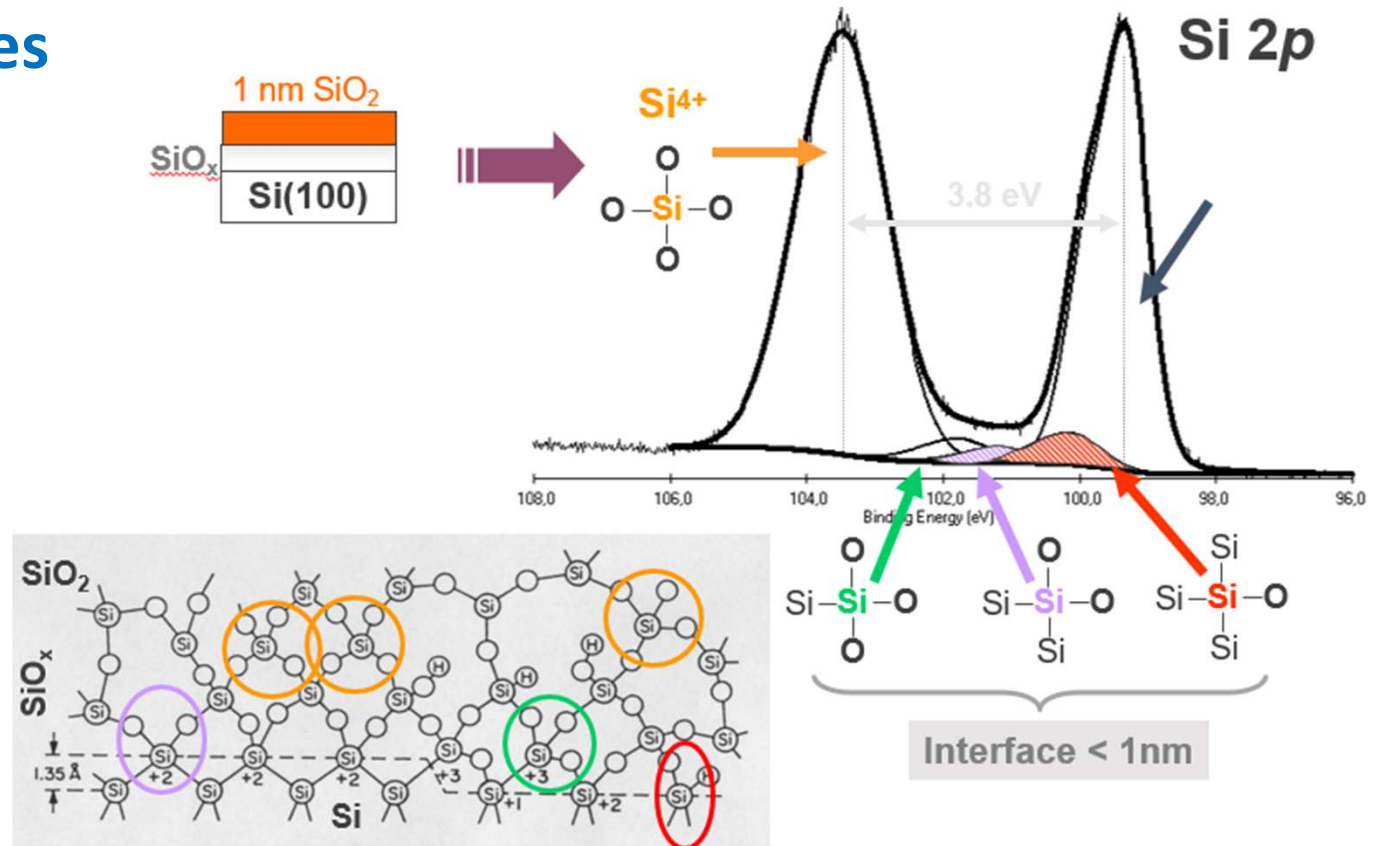
- Downside of XPS:

- Trace analysis 1 at.%
- Depth sensitivity <10 nm



**From XPS to HAXPES**

**From surface to sub-surface and bulk**



P. J. Grunthaner, *J. Appl. Phys.* **61** (2), 629 (1987)

# HAXPES for interfaces at synchrotrons

- **Pro's**

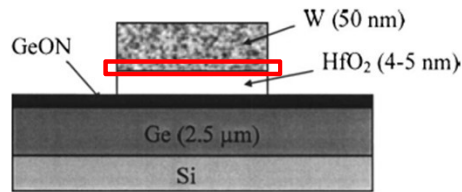
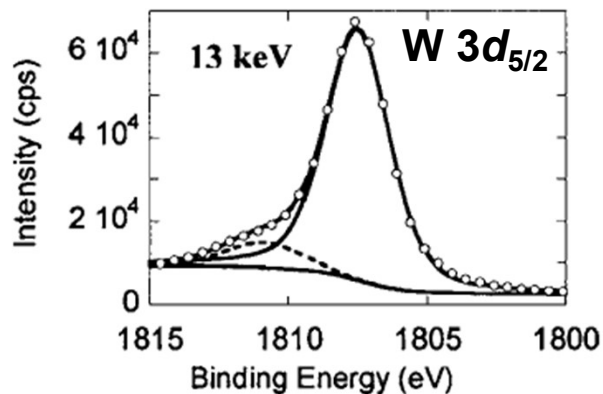
- ✓ Tunable photon energy
- ✓ Large photon flux
- ✓ Energy resolution < 0.25 eV



- **Con's**

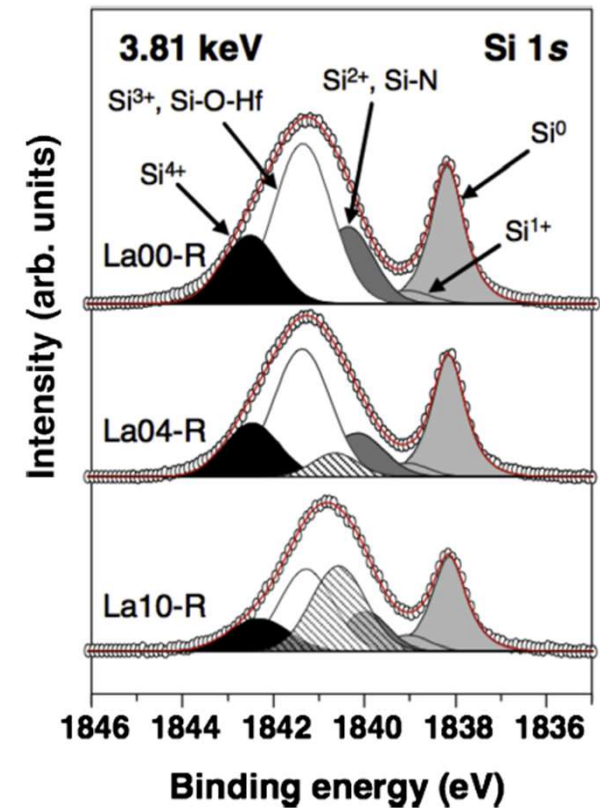
- ⊖ Limited beam time
- ⊖ Predictability of available beamtime
- ⊖ Quantification often complicated

➔ **Not suitable for process developments**

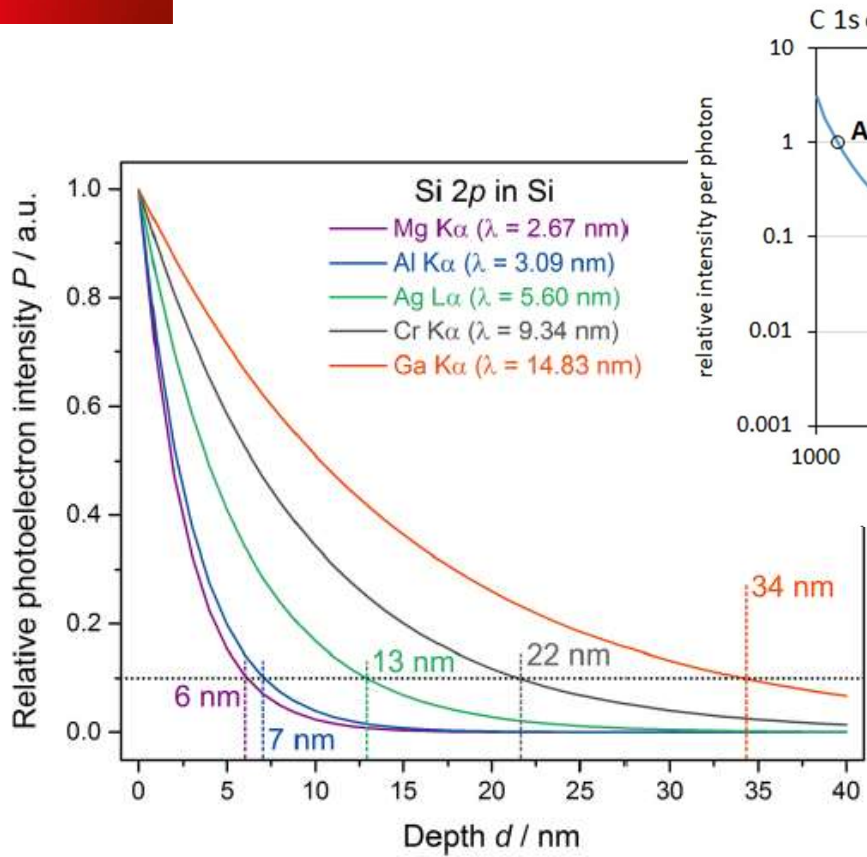


Martinez, Renault, Zegenhagen *et al.*, JVST B. 25, 86 (2006)  
Rubio-Zuazo, Martinez *et al.*, AIP Conf. Proc. 931 (1), 329 (2007)

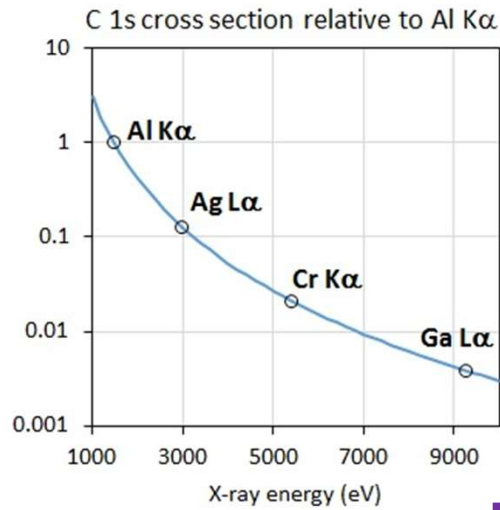
Martinez, Renault, *et al.*, Appl. Surf. Sci. 335, 71 (2015)  
Boujaama, Martinez, Renault, *et al.*, J. Appl. Phys. 111, 054110 (2012)



# Lab-scale HAXPES



Regoutz *et al.*, *Rev. Sci. Instrum* **89**, 073105 (2018).



## Pro's

- ✓ Routine characterization
- ✓ Combined XPS-HAXPES
- ✓ Quantification

## Con's

- ☹ Fixed photon energy
  - Photon flux
  - Energy resolution > 0.5 eV

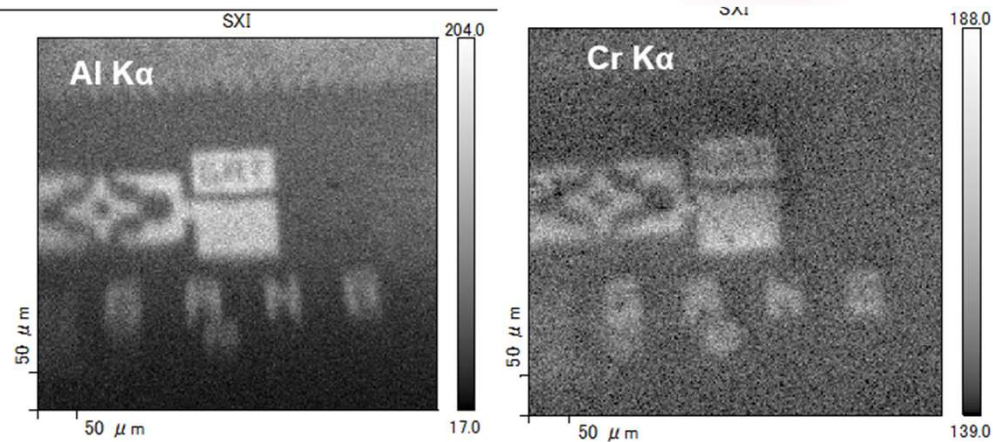
➔ *Suitable for process developments*



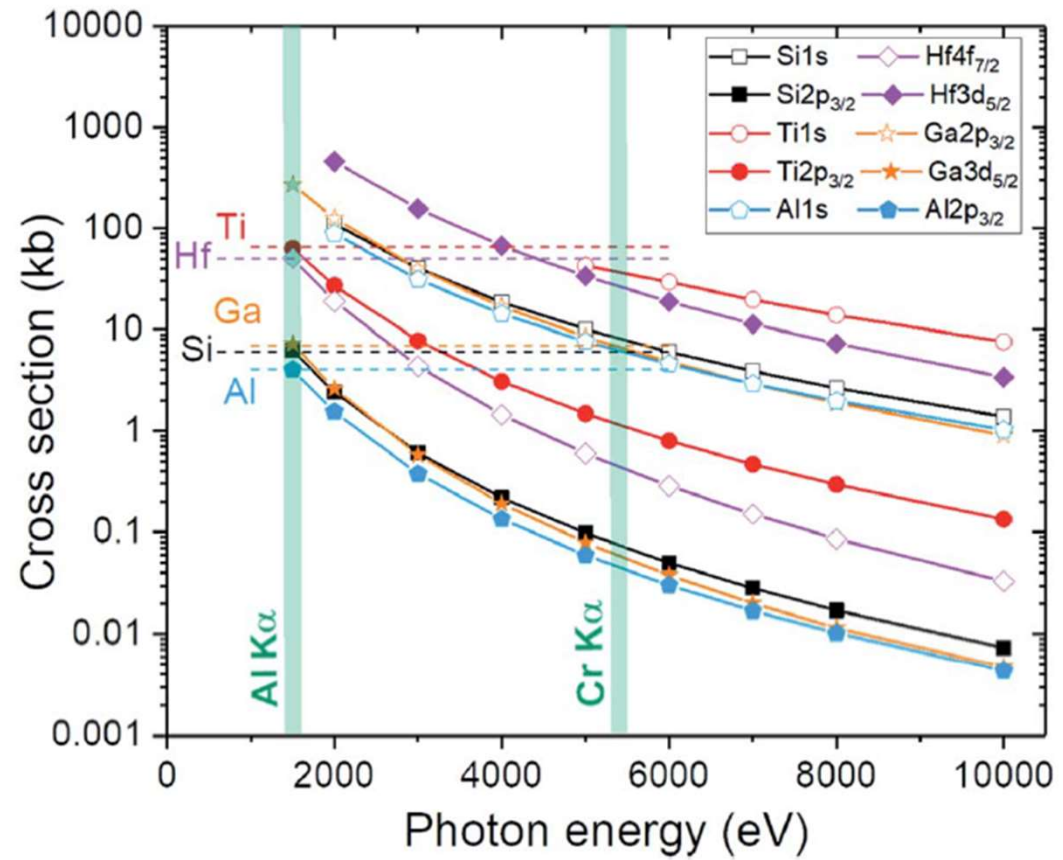
**Poster 009 K. Artyushkova**

# Lab-scale Cr K $\alpha$ HAXPES

- Extended core-line w/o sensitivity loss
- $\times 3$  depth sensitivity
- Confocal  $\mu\text{m}$ -size X-ray sources

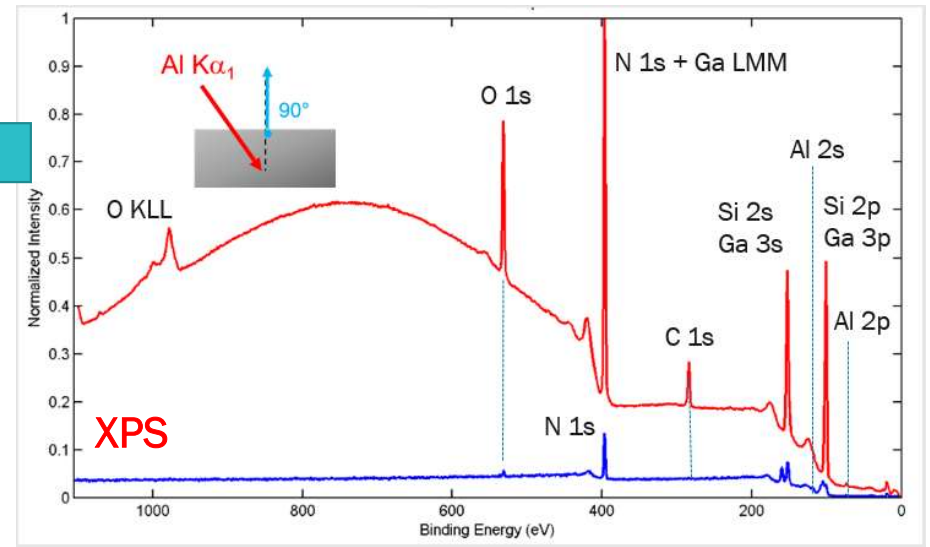
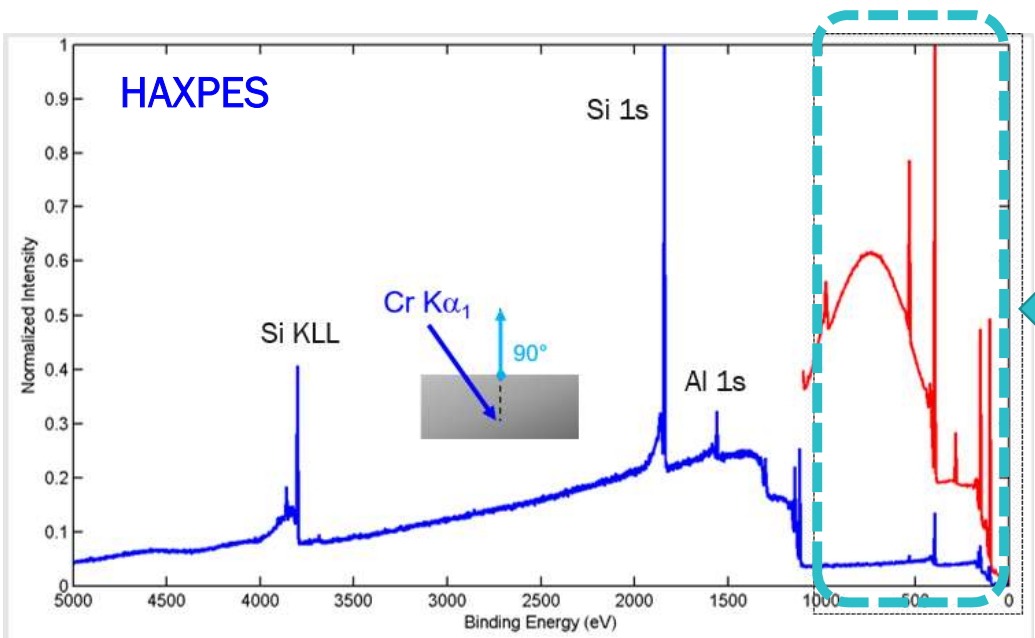


Renault et al., Faraday Disc.(2022)



# Extending core-lines availability

SiN 9 nm
AlN
GaN 2 μm
Si



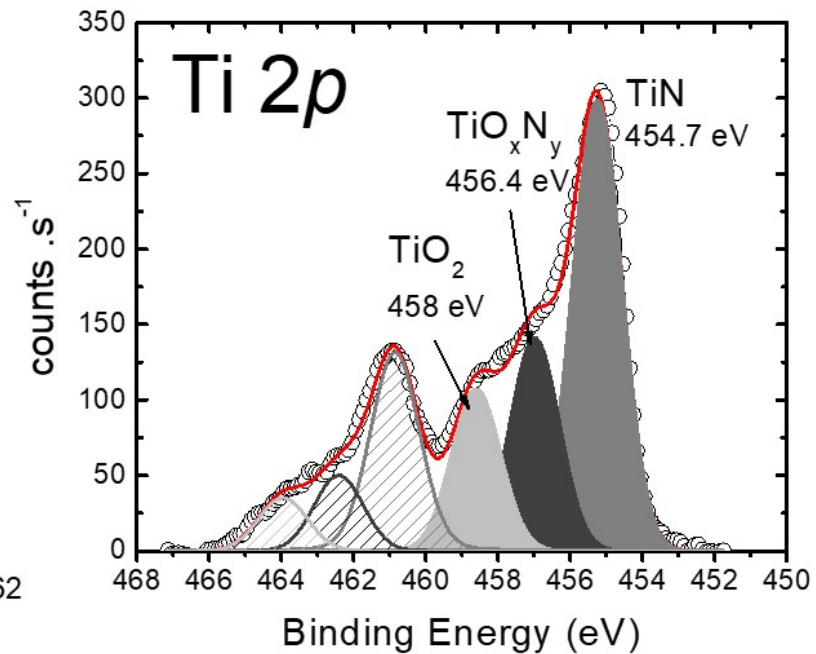
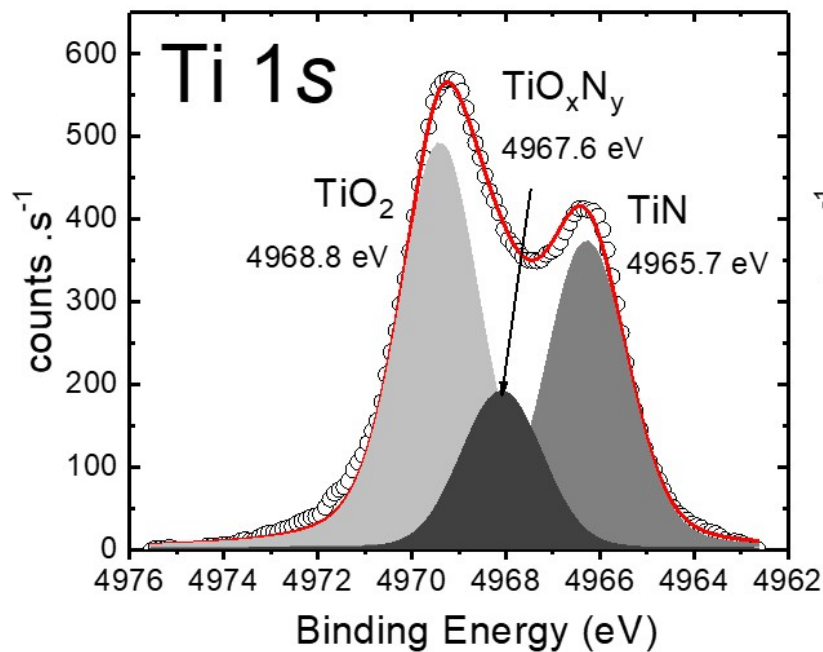
# Extending core-lines availability

Photoelectron	Ti 1s	Ti 2p
Kinetic Energy (KE), eV	449	4962
Material	Pt (TiN)	Pt (TiN)
Inelastic mean-free path, nm	0.77 (1.08)	4.50 (6.93)

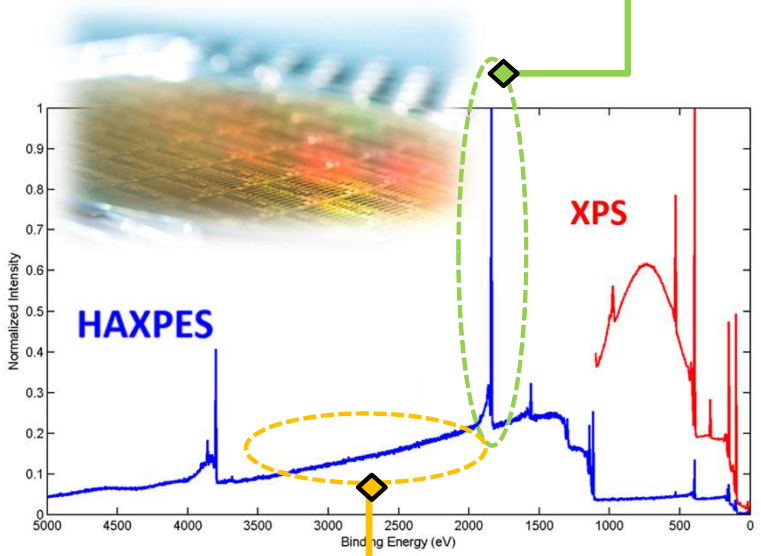
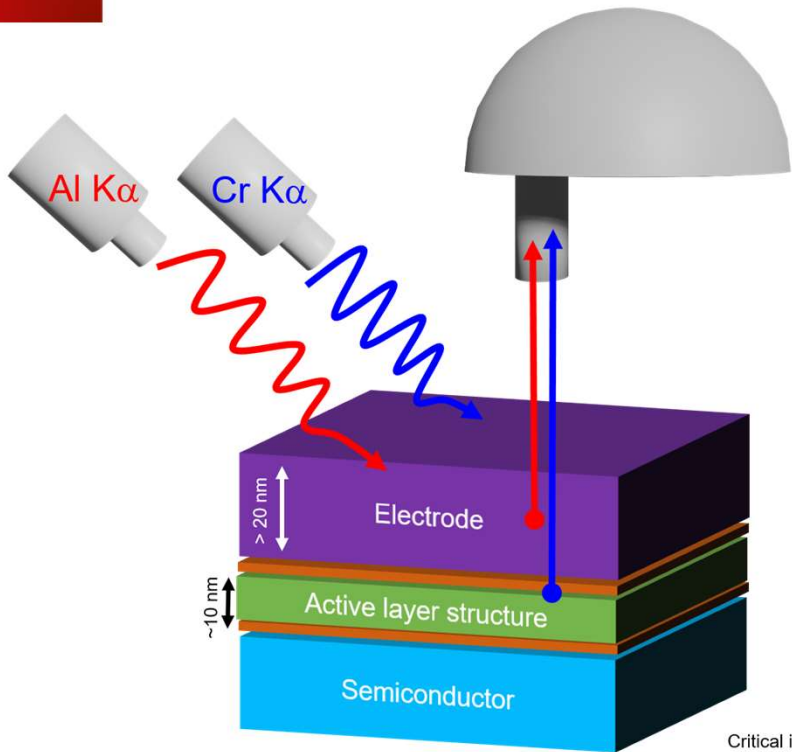
TiO<sub>x</sub> surface layer

TiN 50nm

Si



# Agenda

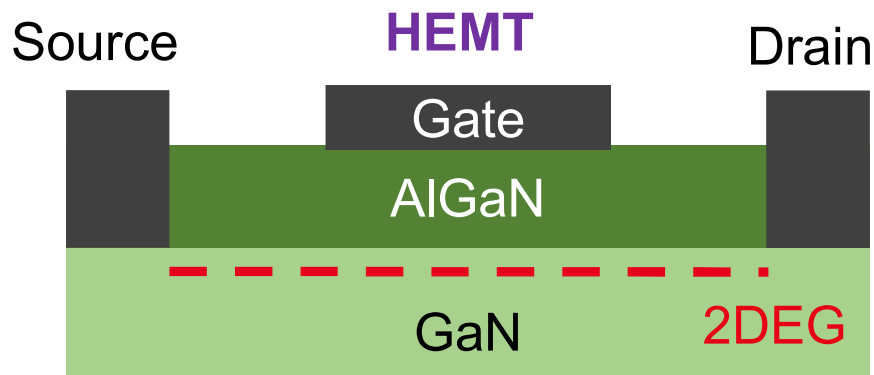


**1. Core-level analysis**  
Chemistry  
at. %  
 $z \sim 3 \times \text{IMFP}$

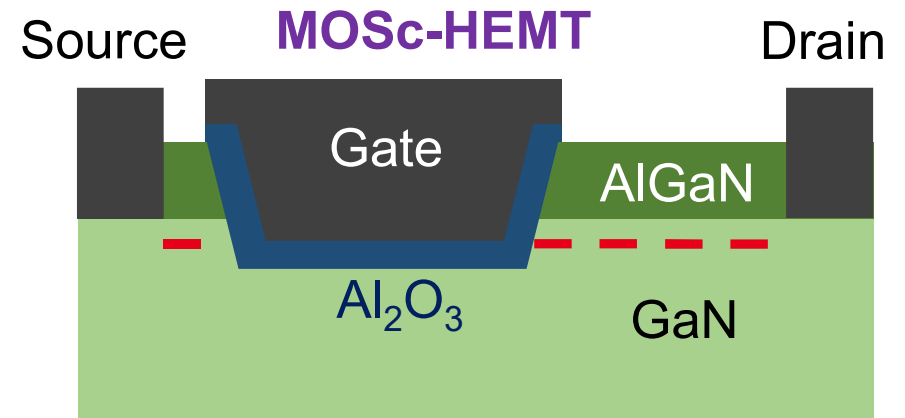
**2. Inelastic background analysis**  
Depth distribution  
 $z \sim 8 \times \text{IMFP}$

Outlook: operando analysis  
In situ bias

## Critical $\text{Al}_2\text{O}_3$ GaN buried interface in HEMTS



- Maximum voltage ( $\sim 650\text{V}$ )
- Low energy loss at ON-state = **Low  $R_{\text{ON}}$**
- OFF-state = negative  $V_{\text{Gate}}$   $\rightarrow$  **Normally-On**

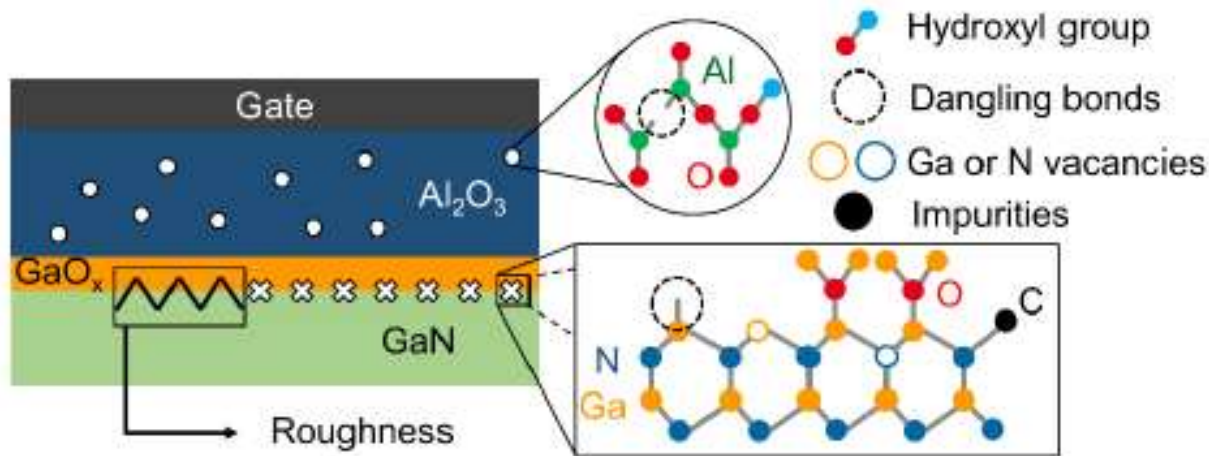


**Normally-Off** by depleting the 2DEG

$\rightarrow$  **MOSc-HEMT**

- AlGaN etch = 2DEG depletion
  - Dielectric deposition (e.g.  $\text{Al}_2\text{O}_3$ )
  - Metal deposition
- ✓ **Positive Threshold voltage ( $V_{\text{TH}}$ )**

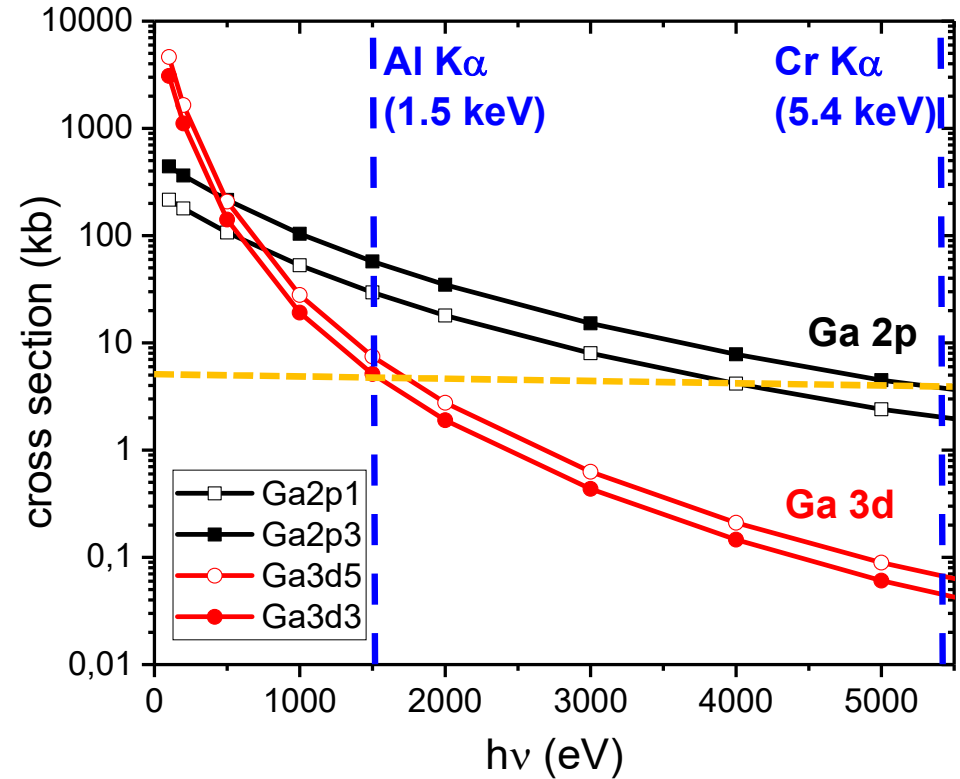
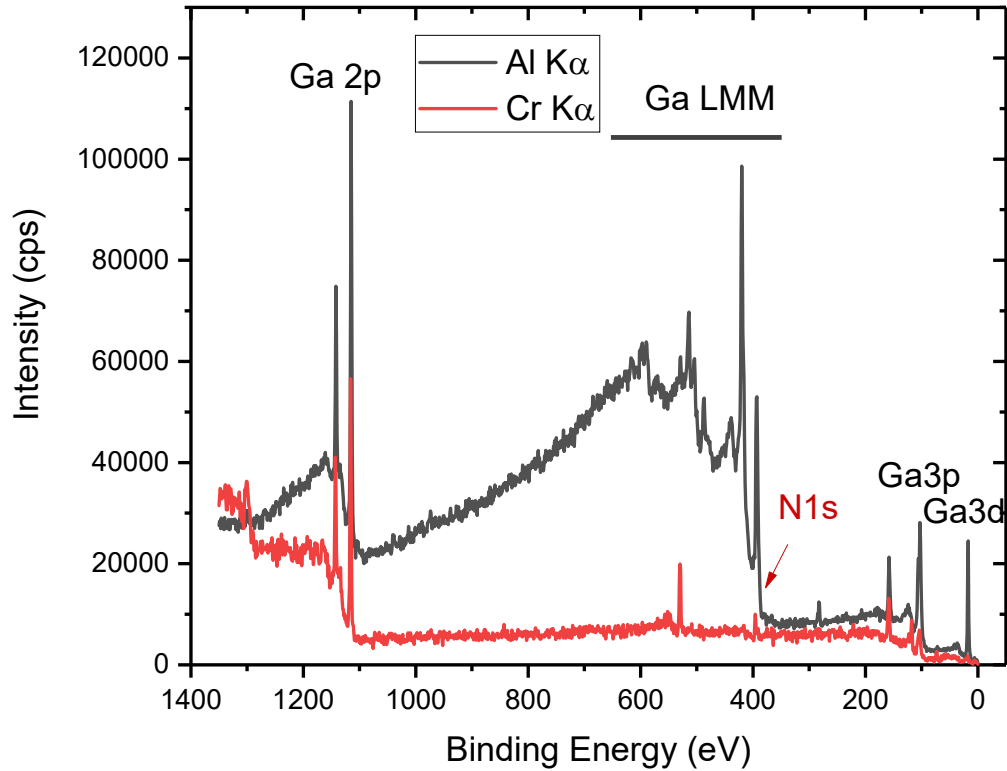
## Critical Al<sub>2</sub>O<sub>3</sub> GaN buried interface in HEMTS



- Ga oxydation  $\Rightarrow$  GaO<sub>x</sub>
- Defects  $\Rightarrow$  dangling bonds, vacancies (Ga, N), impurities
- Roughness
- ✓ Impact on electrical properties ( $V_{TH}$ ,  $\Delta V_{TH}$ ,  $R_{ON}$ )

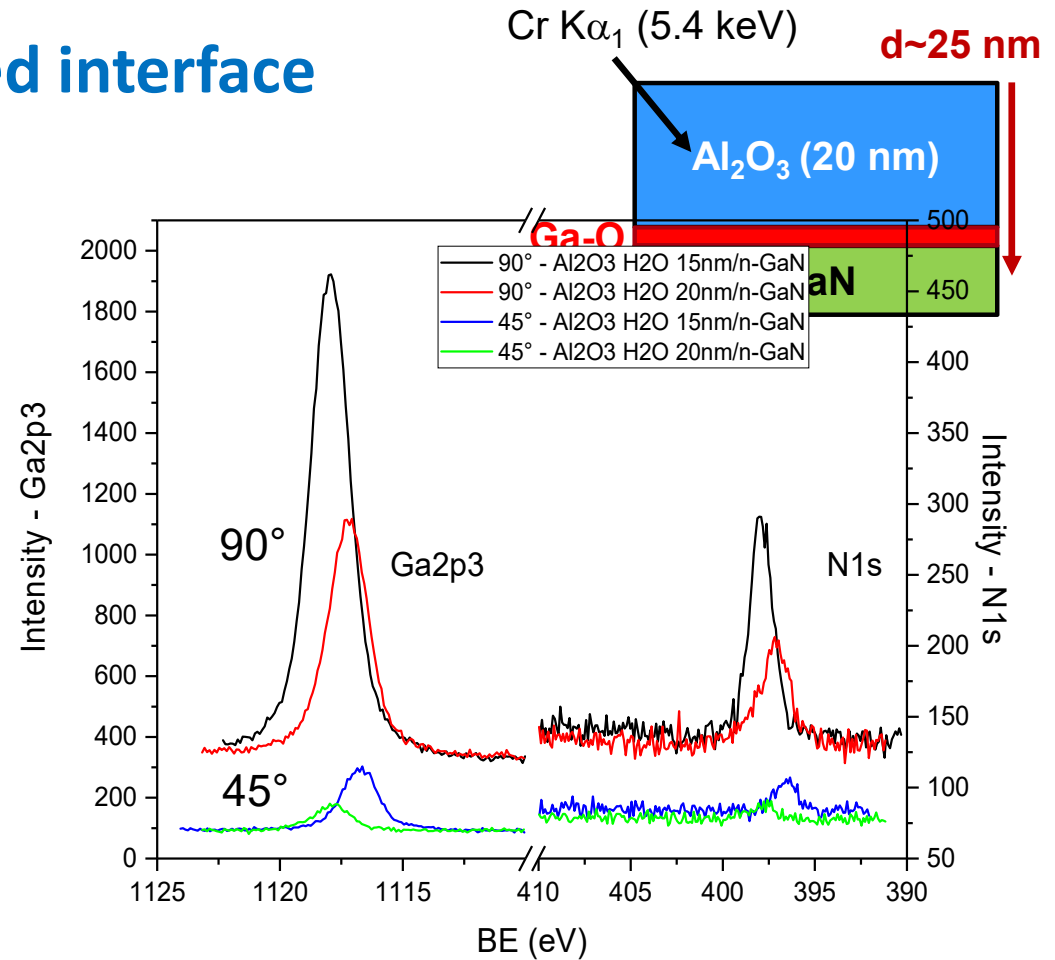
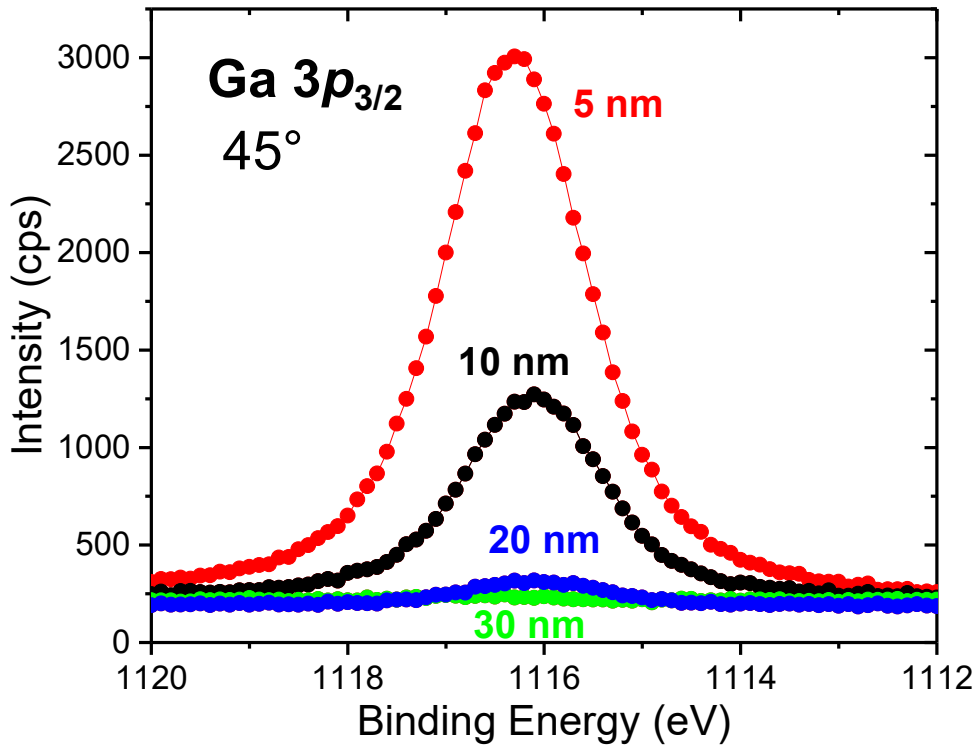
- Al<sub>2</sub>O<sub>3</sub>/GaN interface quality required for good transistor performances

# HAXPES of GaN-based materials



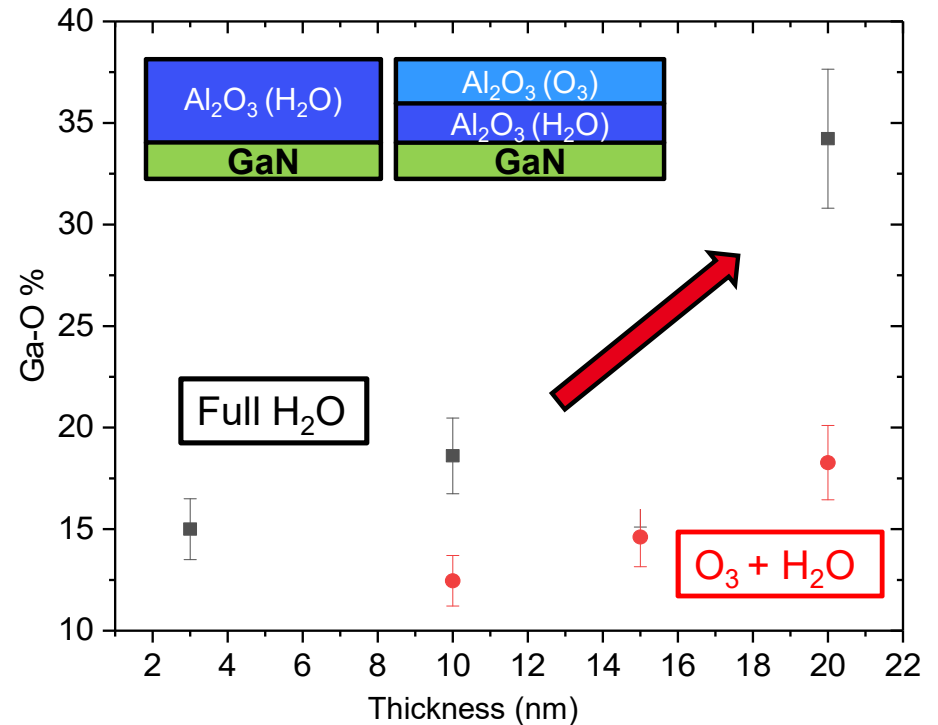
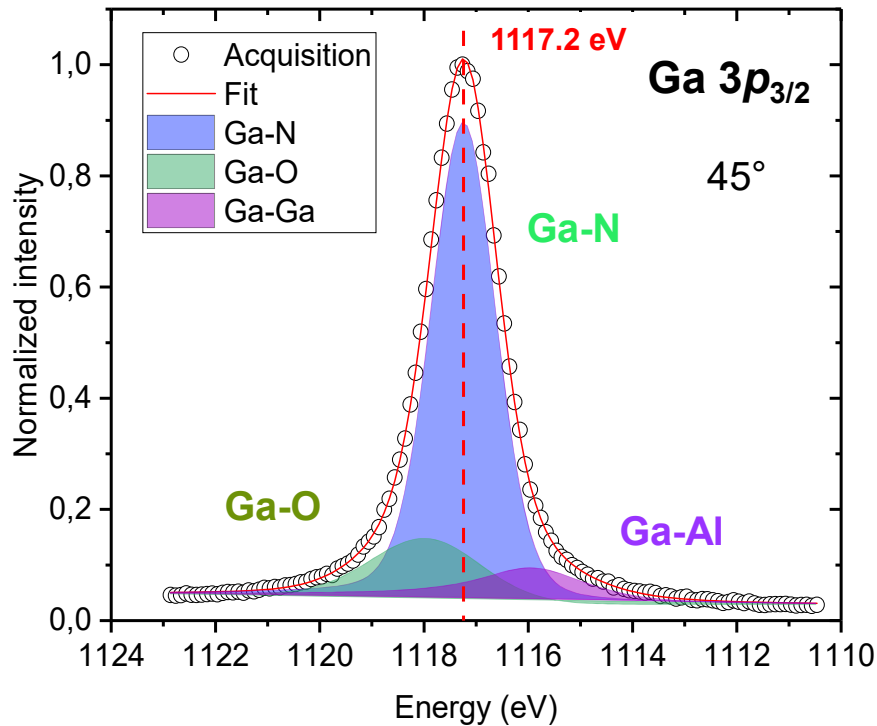
- HAXPES avoids the **overlap between N 1s & Ga LMM**
- **Trade-off** between sensitivity & probing depth with Ga 2p/Ga 3d

# HAXPES of Al<sub>2</sub>O<sub>3</sub>-GaN buried interface



- Investigate the GaN interface with a **20 nm-thick Al<sub>2</sub>O<sub>3</sub>** upper layer

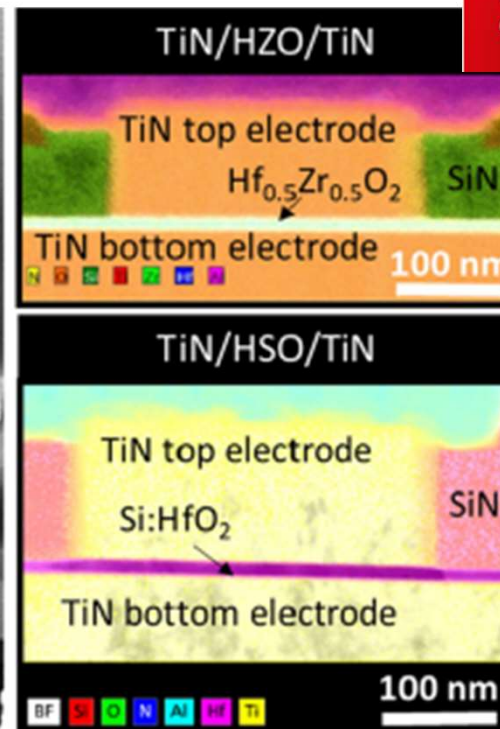
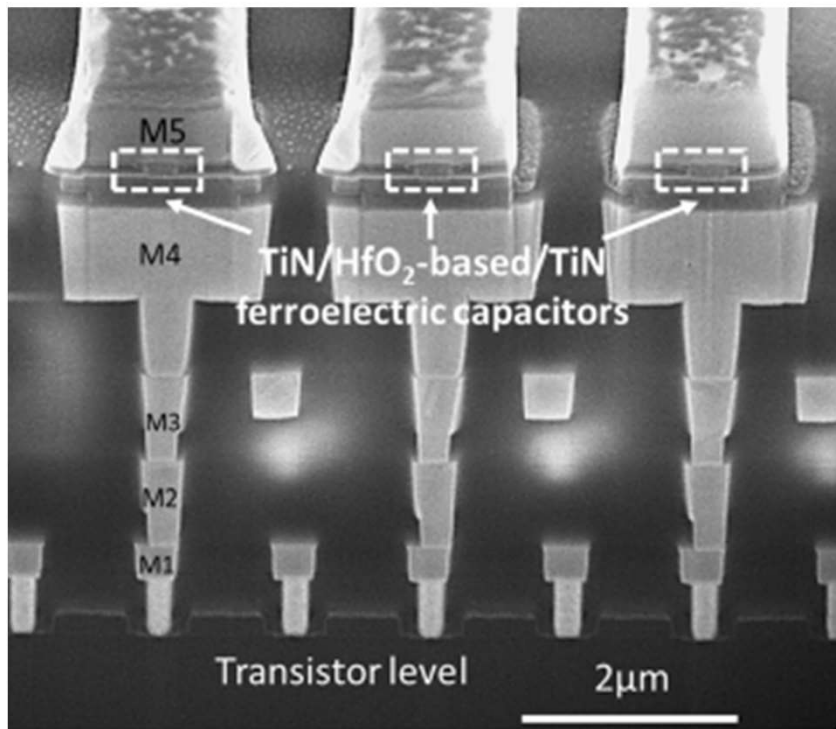
# HAXPES of Al<sub>2</sub>O<sub>3</sub>-GaN buried interface



- Impact of alumina thickness & processing on GaN oxidation
- Increase of Ga-O bonds at the GaN surface with increasing Al<sub>2</sub>O<sub>3</sub> thickness

# HfO<sub>2</sub> stacks for FERAMs

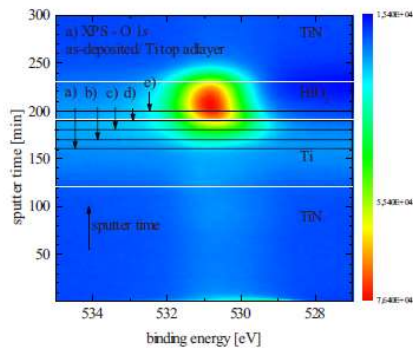
- **Ferroelectric** HfO<sub>2</sub> phase
- Oxygen vacancies or Si/La doping stabilize the ferro phase



# HfO<sub>2</sub> stacks for FERAMs

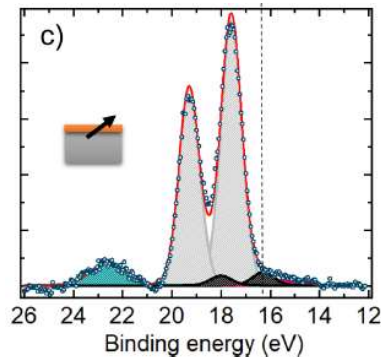
- Ferroelectric HfO<sub>2</sub> phase
- Oxygen vacancies or Si/La doping stabilize the ferro phase
- **Analysis of HfO<sub>2</sub>/top electrode interface:** different approaches

## XPS sputter profiling



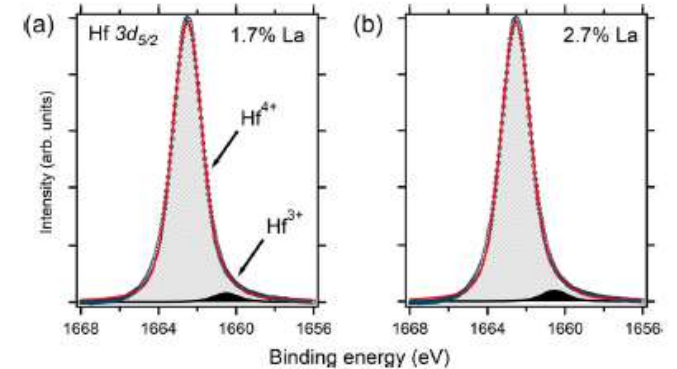
Walczyk *et al.*, J. Vac. Sci. Technol. B **29** (2011)

## XPS with ultra-thin electrode



Hamouda *et al.*, J. Appl. Phys. **127**,064105 (2020)

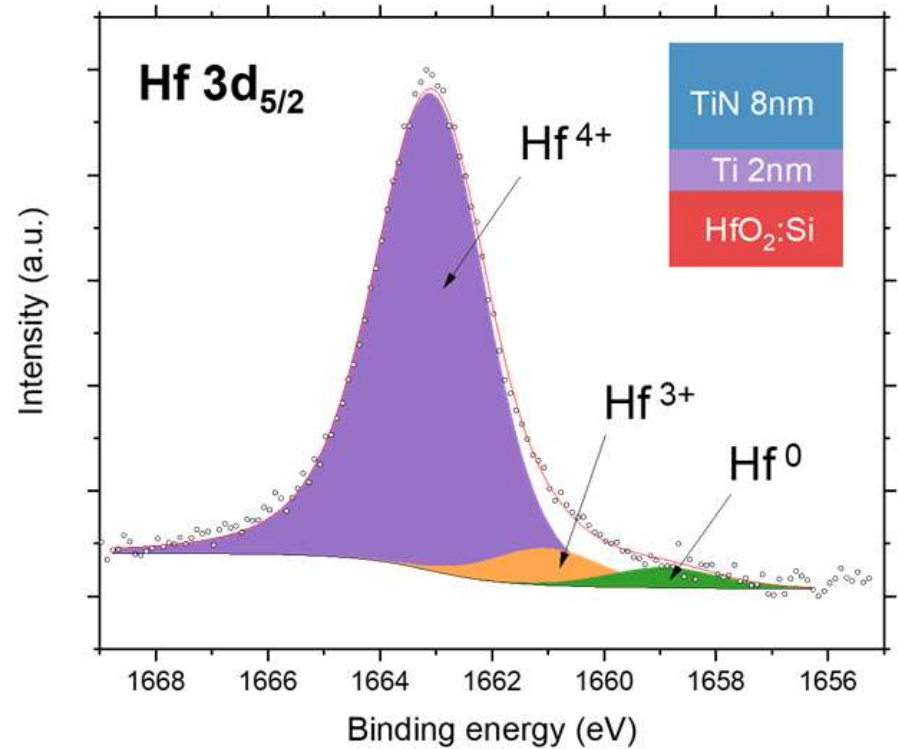
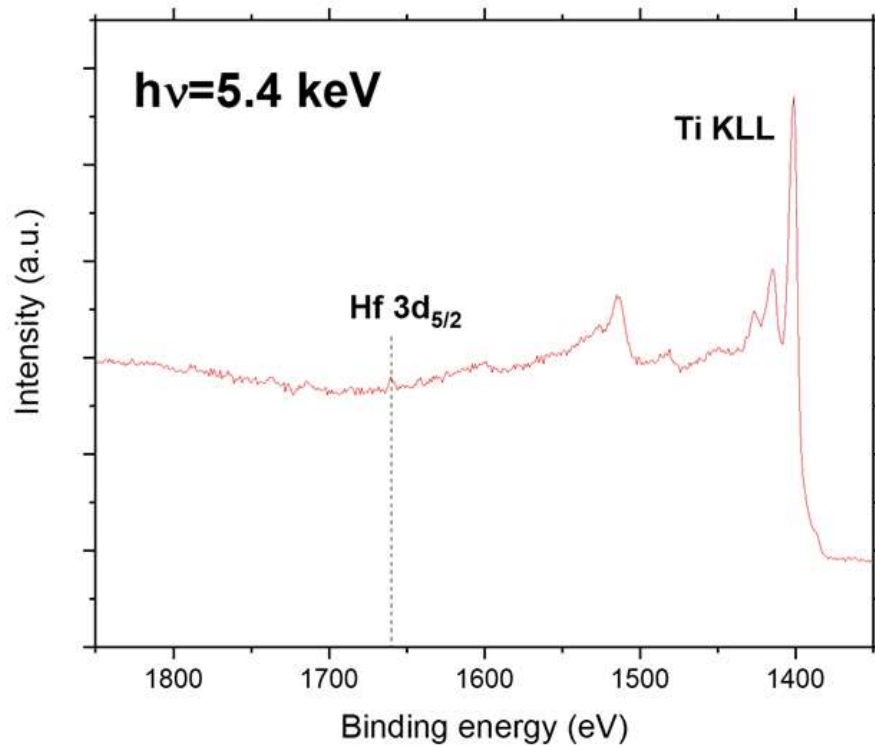
## HAXPES with synchrotron radiation



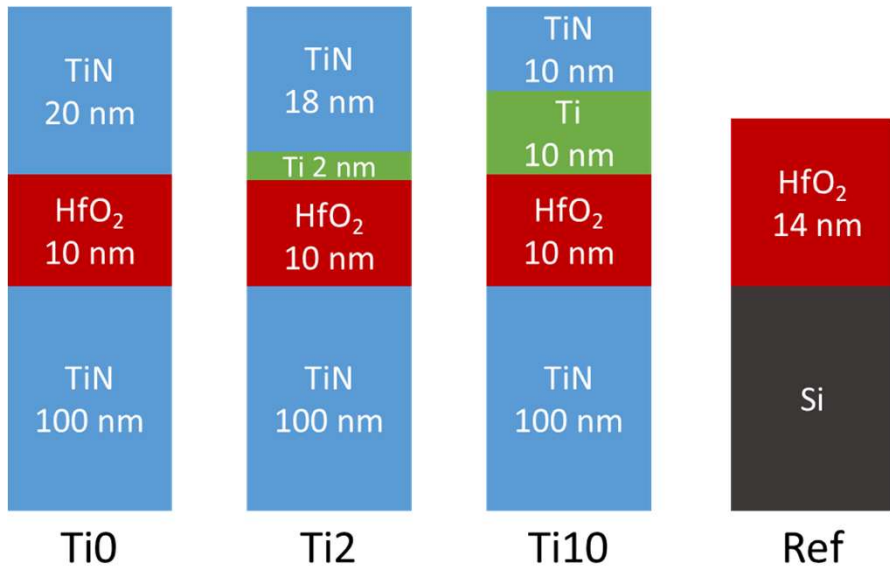
Hamouda *et al.*, Appl. Phys. Lett. **116**, 252903 (2020)

# HfO<sub>2</sub> stacks for FERAMs

- Analysis of HfO<sub>2</sub>/top electrode interface: lab-scale Cr K $\alpha$  HAXPES



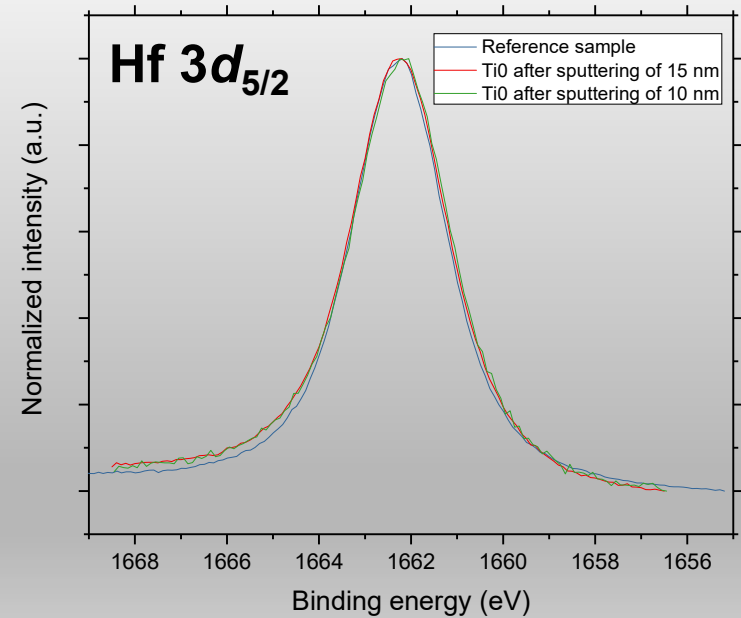
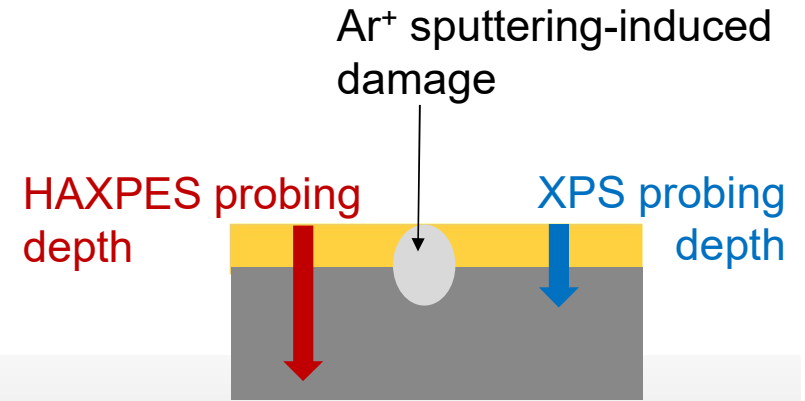
# HAXPES of HfO<sub>2</sub>-TE interface



$\lambda_{\text{Hf}3d}(\text{TiN}) = 5.5 \text{ nm} \rightarrow \text{Probing depth} < 16 \text{ nm}$



*Partial sputter of the top electrode*

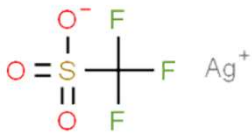


# HAXPES quantification: elemental RSFs

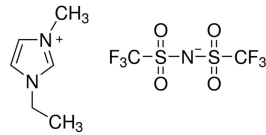
- Pure element RSFs (PERSF) derived based on the intensity ratios with respect to pure silver:

$$\frac{RSF_{transition}}{RSF_{Ag3d}} = \frac{\frac{Intensity_{transition}}{TFC_{transition}} \times Asymetry_{transition}}{\frac{Intensity_{Ag3d}}{TFC_{Ag3d}} \times Asymetry_{Ag3d}}$$

- $RSF_{F1s} = 1$
- PERSF for 54 elements



Silver (trifluoromethyl)sulfonate  
AgCF3SO3



EMIM TFSI  
C8H11F6N3O4S2

Periodic Table of the Elements

1 IA H Hydrogen 1.008	2 IIA He Helium 4.003																	18 VIIIA Ar Argon 39.948
3 IIIA Li Lithium 6.941	4 IIA Be Beryllium 9.012											13 IIIA B Boron 10.811	14 IVA C Carbon 12.011	15 VA N Nitrogen 14.007	16 VIA O Oxygen 15.999	17 VIIA F Fluorine 18.998	18 VIIIA Ne Neon 20.180	
11 IB Na Sodium 22.990	12 IIB Mg Magnesium 24.305	3 IIIB Sc Scandium 44.956	4 IVB Ti Titanium 47.867	5 VB V Vanadium 50.942	6 VIB Cr Chromium 51.996	7 VIIB Mn Manganese 54.938	8 VIII Fe Iron 55.845	9 VIII Co Cobalt 58.933	10 VIII Ni Nickel 58.693	11 IB Cu Copper 63.546	12 IIB Zn Zinc 65.38	13 IIIA Al Aluminum 26.982	14 IVA Si Silicon 28.086	15 VA P Phosphorus 30.974	16 VIA S Sulfur 32.06	17 VIIA Cl Chlorine 35.453	18 VIIIA Ar Argon 39.948	
19 IA K Potassium 39.098	20 IIA Ca Calcium 40.078	21 IIIB Sc Scandium 44.956	22 IVB Ti Titanium 47.867	23 VB V Vanadium 50.942	24 VIB Cr Chromium 51.996	25 VIIB Mn Manganese 54.938	26 VIII Fe Iron 55.845	27 VIII Co Cobalt 58.933	28 VIII Ni Nickel 58.693	29 IB Cu Copper 63.546	30 IIB Zn Zinc 65.38	31 IIIA Ga Gallium 69.723	32 IVA Ge Germanium 72.63	33 VA As Arsenic 74.922	34 VIA Se Selenium 78.96	35 VIIA Br Bromine 79.904	36 VIIIA Kr Krypton 83.798	
37 IA Rb Rubidium 85.468	38 IIA Sr Strontium 87.62	39 IIIB Y Yttrium 88.906	40 IVB Zr Zirconium 91.224	41 VB Nb Niobium 92.906	42 VIB Mo Molybdenum 95.94	43 VIIB Tc Technetium 98.907	44 VIII Ru Ruthenium 101.07	45 VIII Rh Rhodium 102.905	46 VIII Pd Palladium 106.42	47 IB Ag Silver 107.868	48 IIB Cd Cadmium 112.414	49 IIIA In Indium 114.818	50 IVA Sn Tin 118.710	51 VA Sb Antimony 121.757	52 VIA Te Tellurium 127.6	53 VIIA I Iodine 126.905	54 VIIIA Xe Xenon 131.29	
55 IA Cs Cesium 132.905	56 IIA Ba Barium 137.327	57-71 Lanthanide Series	72 IVB Hf Hafnium 178.49	73 VB Ta Tantalum 180.948	74 VIB W Tungsten 183.84	75 VIIB Re Rhenium 186.207	76 VIII Os Osmium 190.23	77 VIII Ir Iridium 192.22	78 VIII Pt Platinum 195.084	79 IB Au Gold 196.967	80 IIB Hg Mercury 200.592	81 IIIA Tl Thallium 204.383	82 IVA Pb Lead 207.2	83 VA Bi Bismuth 208.980	84 VIA Po Polonium 209	85 VIIA At Astatine 209	86 VIIIA Rn Radon 222.018	
87 IA Fr Francium 223.020	88 IIA Ra Radium 226.025	89-103 Actinide Series	104 IVB Rf Rutherfordium 261	105 VB Db Dubnium 262	106 VIB Sg Seaborgium 263	107 VIIB Bh Bohrium 264	108 VIII Hs Hassium 265	109 VIII Mt Meitnerium 266	110 VIII Ds Darmstadtium 267	111 IB Rg Roentgenium 268	112 IIB Cn Copernicium 269	113 IIIA Nh Nihonium 270	114 IVA Fl Flerovium 271	115 VA Mc Moscovium 272	116 VIA Lv Livermorium 273	117 VIIA Ts Tennessine 274	118 VIIIA Og Oganesson 276	
57 Lanthanide Series La Lanthanum 138.905	58 Ce Cerium 140.116	59 Pr Praseodymium 140.908	60 Nd Neodymium 144.242	61 Pm Promethium 144.913	62 Sm Samarium 150.36	63 Eu Europium 151.964	64 Gd Gadolinium 157.25	65 Tb Terbium 158.925	66 Dy Dysprosium 162.502	67 Ho Holmium 164.930	68 Er Erbium 167.259	69 Tm Thulium 168.934	70 Yb Ytterbium 173.054	71 Lu Lutetium 174.967				
89 Actinide Series Ac Actinium 227.028	90 Th Thorium 232.038	91 Pa Protactinium 231.036	92 U Uranium 238.029	93 Np Neptunium 237.048	94 Pu Plutonium 244.064	95 Am Americium 243.061	96 Cm Curium 247.070	97 Bk Berkelium 247.070	98 Cf Californium 251.080	99 Es Einsteinium 252.083	100 Fm Fermium 257.095	101 Md Mendelevium 258	102 No Nobelium 259.101	103 Lr Lawrencium [262]				

# HAXPES quantification: elemental RSFs for compounds

SiC	Si at. %	% error
Si1s	51.0	2%
Si2s	48.2	-3%
Si2p	51.4	3%

Si <sub>3</sub> N <sub>4</sub>	Si at. %	% error
Si1s	43.4	1%
Si2s	40.4	-6%
Si2p	43.2	0%

➡ Average error is less than 5%

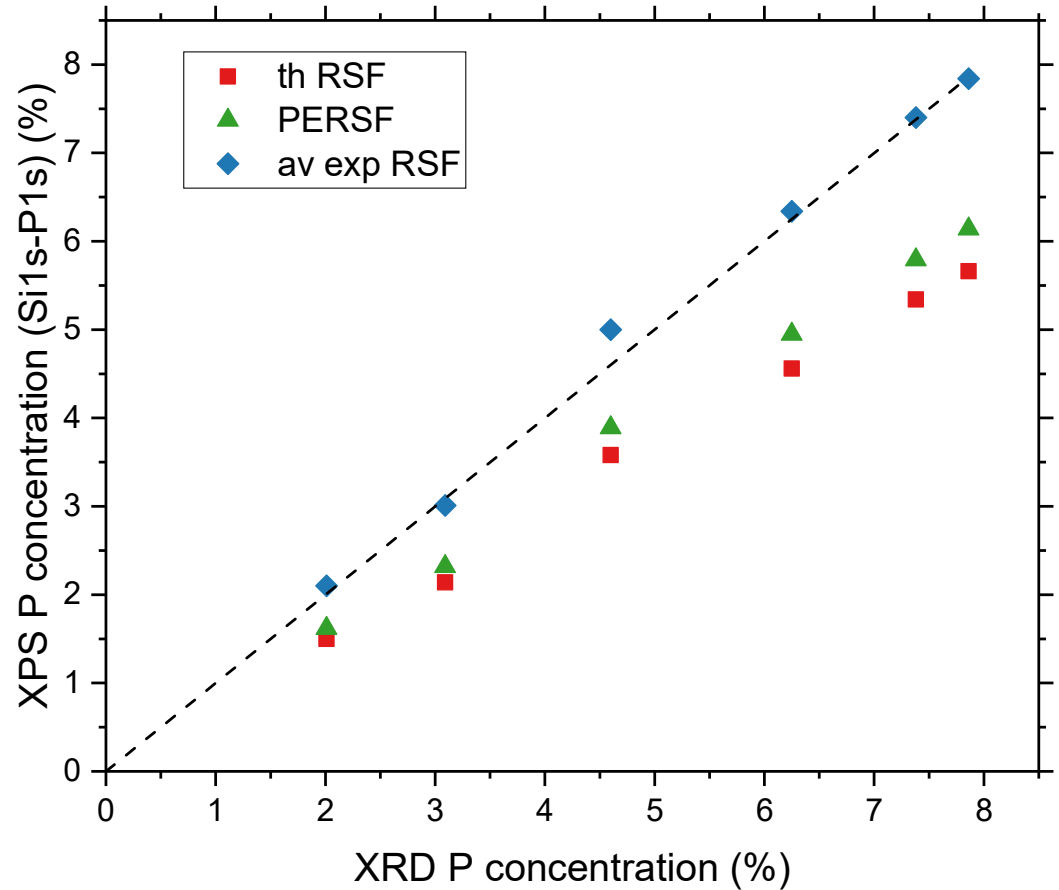
MoSe <sub>2</sub>	Mo at. %	% error
2s-2s	31.7	-5%
2p-2p	30.0	-10%
3p-3p	31.1	7%

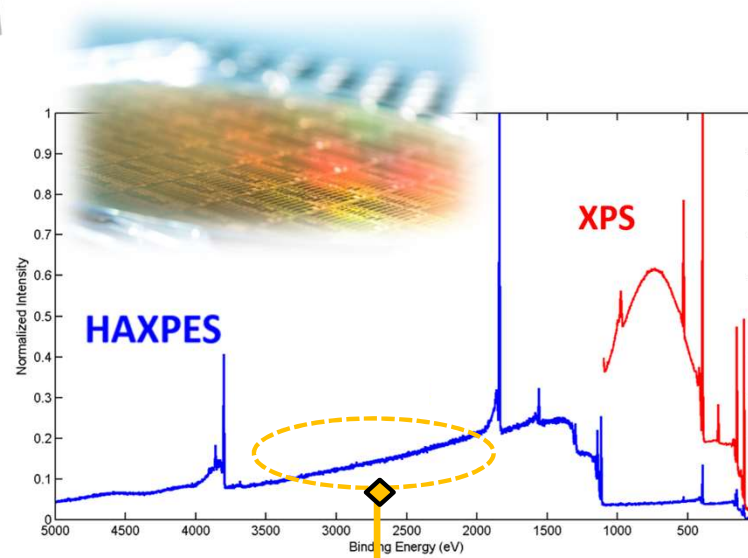
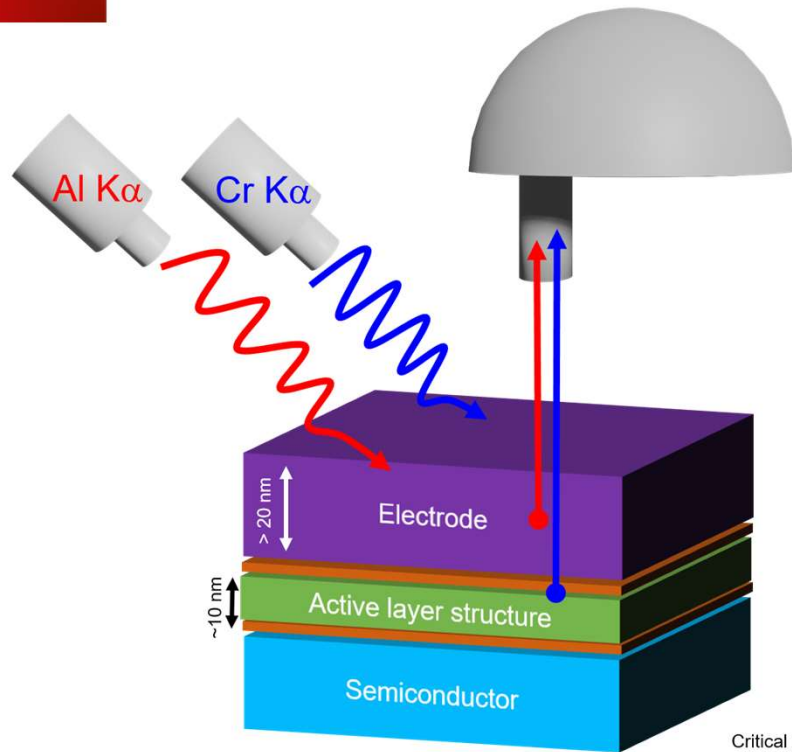
Al <sub>2</sub> O <sub>3</sub>	Al at. %	% error
Al1s	38.1	5%
Al2s	35.8	10%
Al2p	37.8	-6%

AlN	Al at. %	% error
Al1s	50.2	0%
Al2s	48.1	-4%
Al2p	49.4	1%

## HAXPES quantification: average experimental RSFs

- Si:P layers quantified by XRD
- Use of average experimental RSF's (compounds derived)





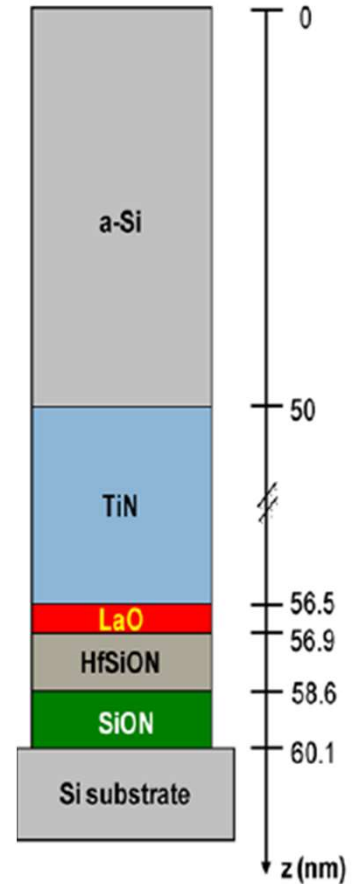
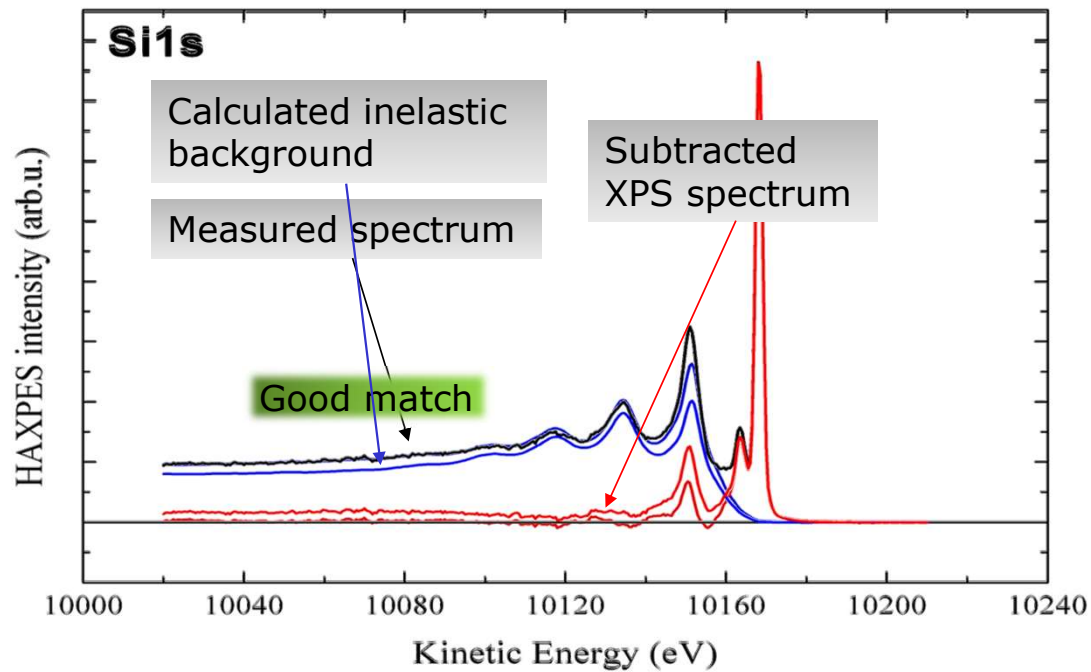
## 2. Inelastic background analysis

Depth distribution

$z \sim 8 \times \text{IMFP}$

# Inelastic background analysis in HAXPES

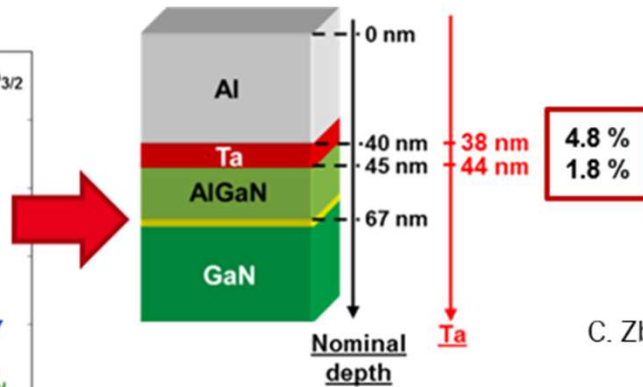
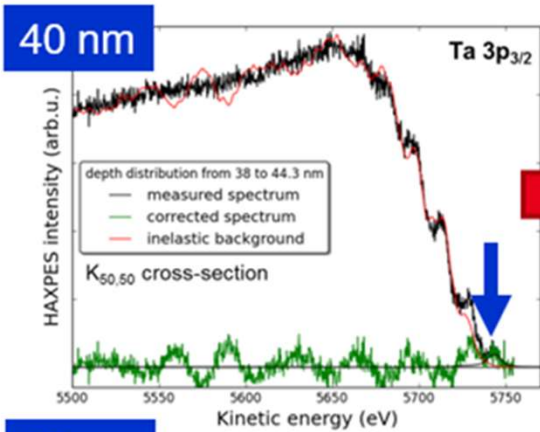
**XPS** S. Tougaard, J. Vac. Sci. Technol. A, 5, 1275 (1997)  
 S. Tougaard, Surf. Interface Anal. 2018; **50**: 857 (2019)  
 S. Tougaard, J. Vac. Sci. Technol. A, 39, 011201 (2021)



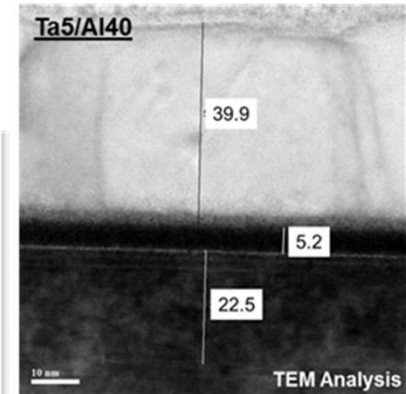
## HAXPES

Risterucci, Martinez, Tougaard, *Appl. Phys. Lett.* **104** (5) (2014)  
 Risterucci, Renault, Tougaard, *Appl. Surf. Sci.* **402** 78 (2017)  
 Zborovski, Renault, Tougaard, *Appl. Surf. Sci.* **432** 60 (2018)  
 Zborovski, Renault, Tougaard, *J. Appl. Phys.* **124** 085115 (2018)  
 Zborovski, Tougaard, *Surf. Interface Anal.* 2019; **51**: 857 (2019)  
 Spencer, Shard, Tougaard, *Appl. Surf. Sci.* **541** 148635 (2021)

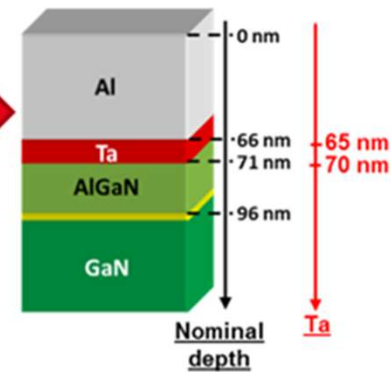
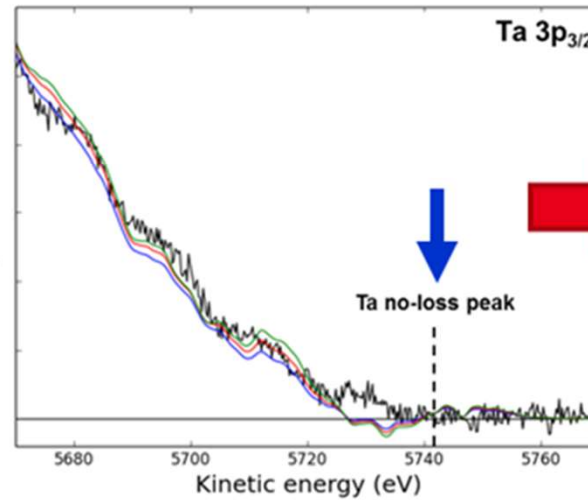
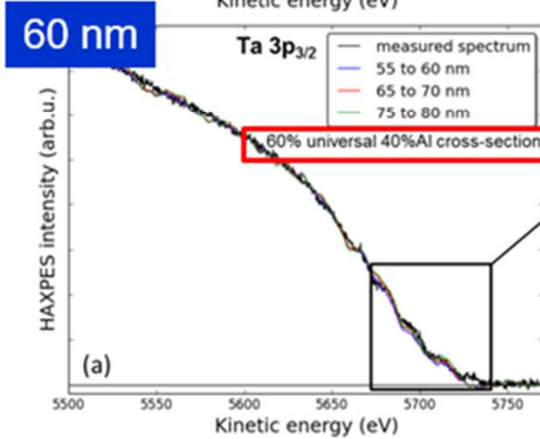
# Inelastic background analysis in HAXPES



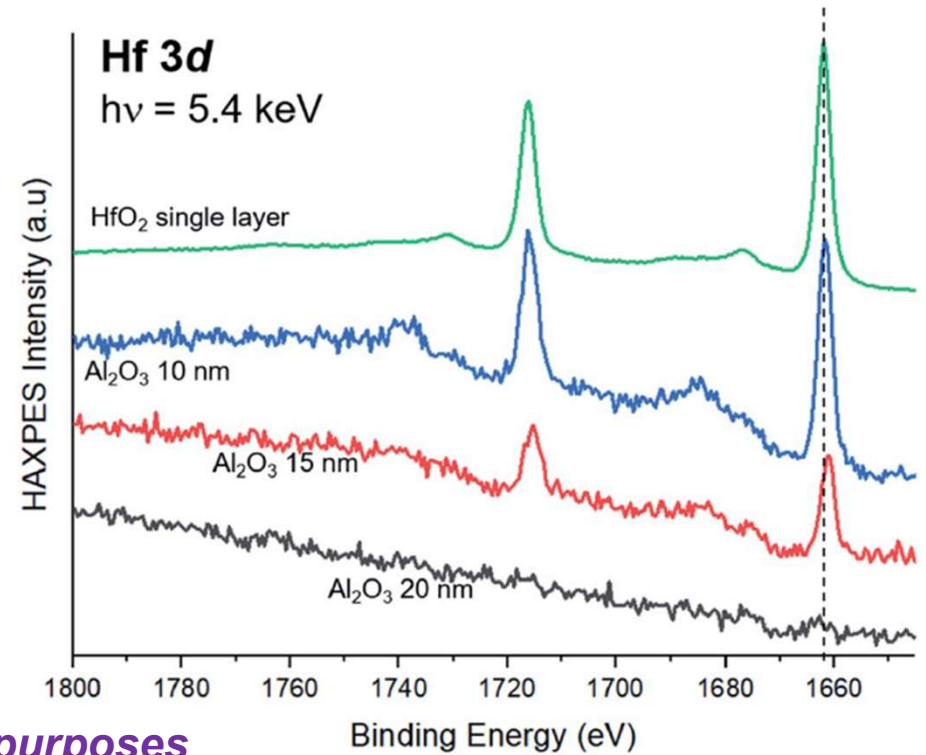
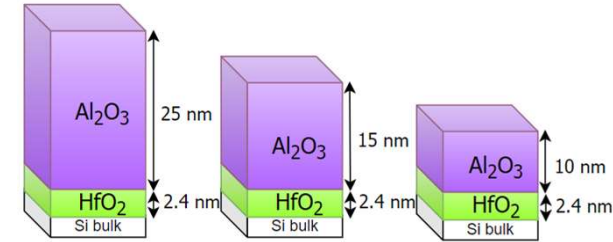
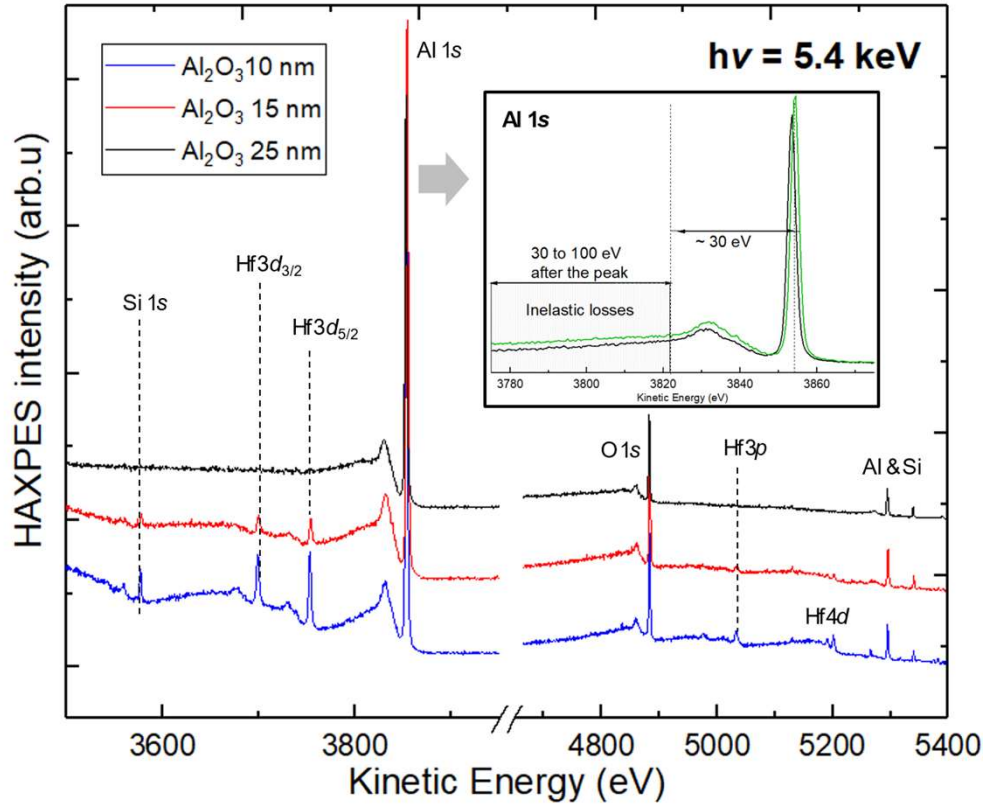
SPring 8  
BL15XU  
 $h\nu=8$  keV



C. Zborowski, O. Renault, S. Tougaard, *Appl. Surf. Sci.* **432** 60 (2018)

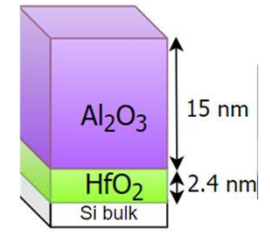
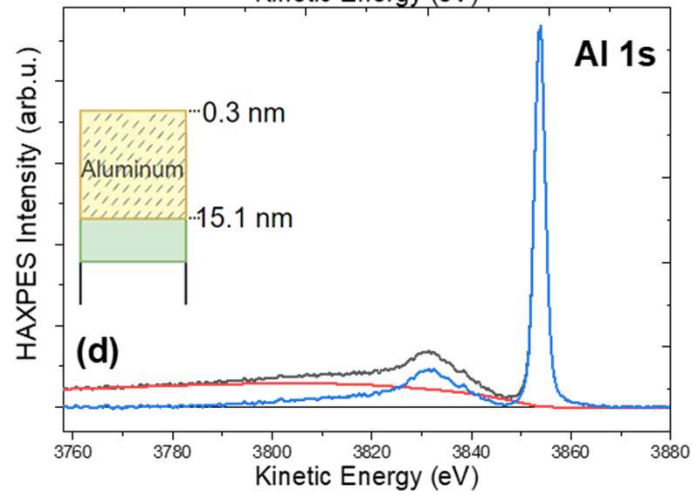
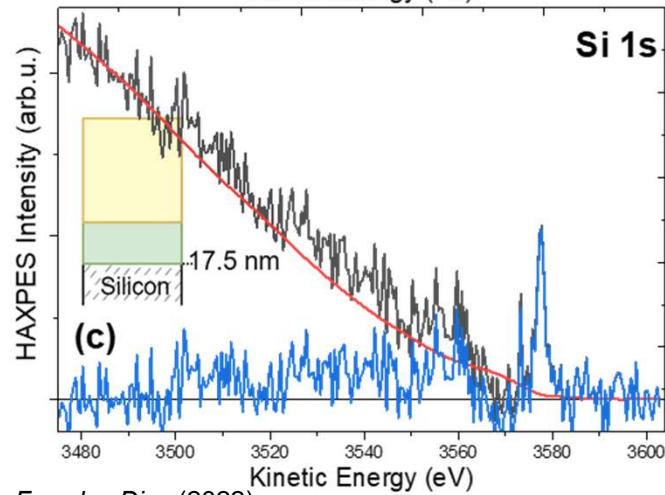
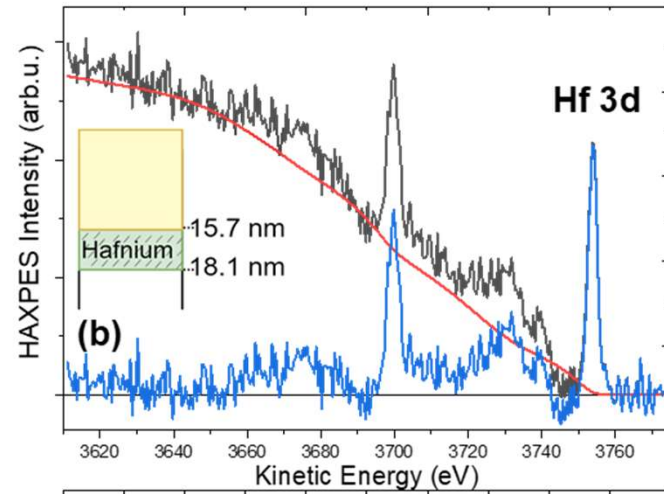
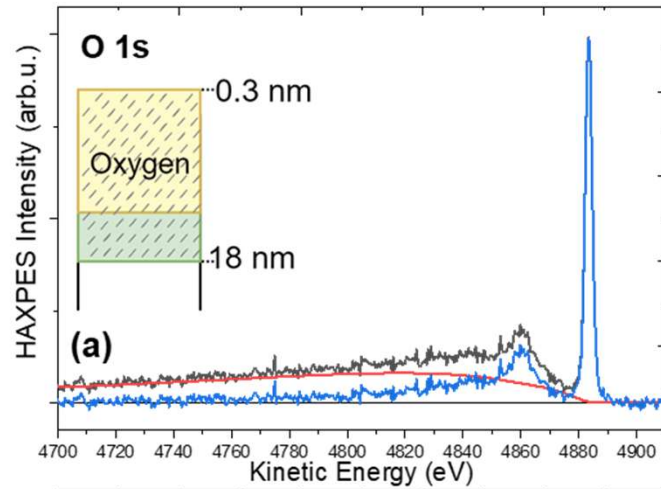


# Background analysis in Cr K $\alpha$ HAXPES

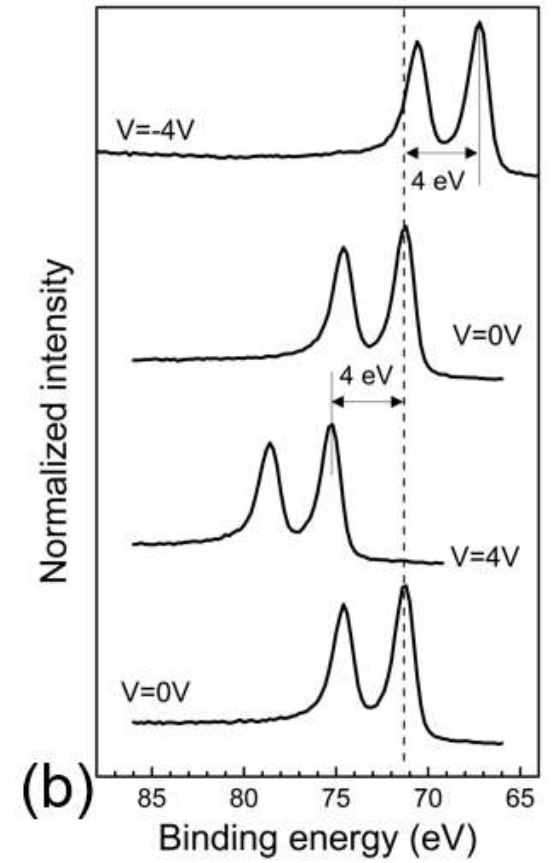
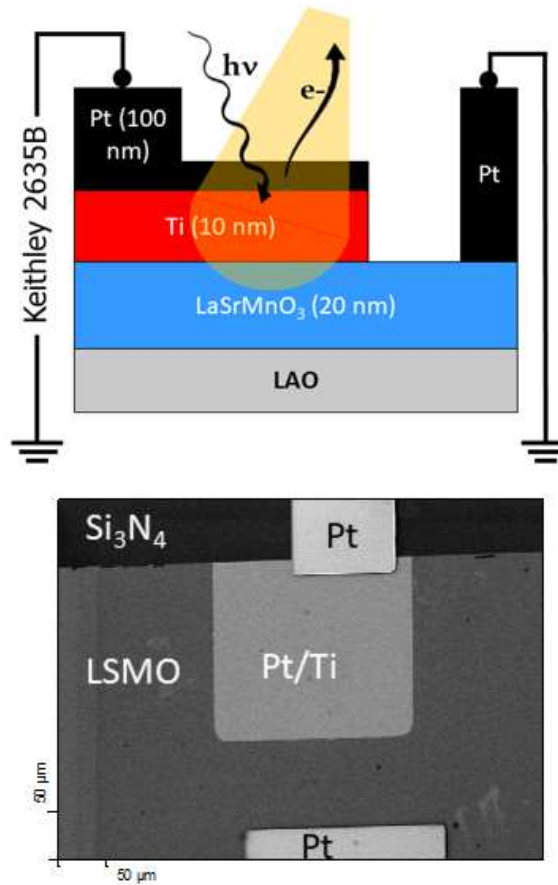
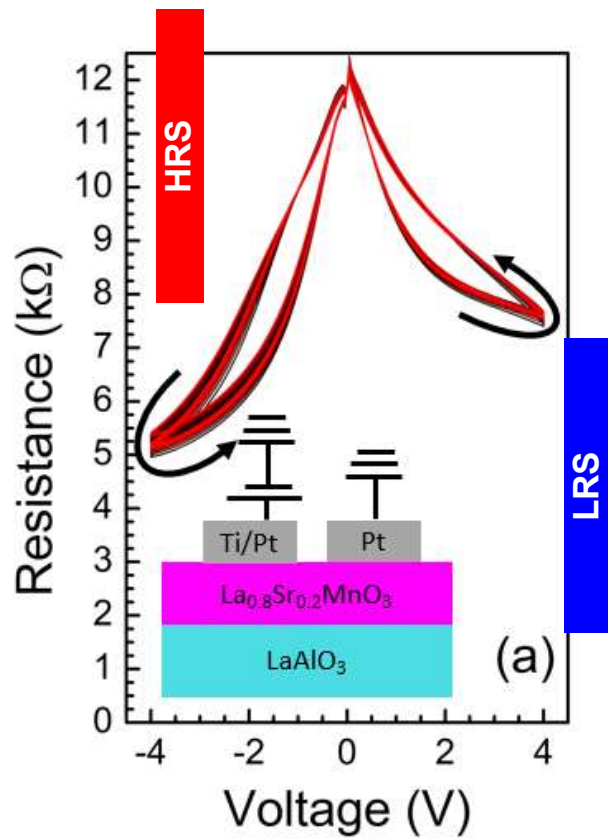


➔ **Testing accuracy of IBA towards metrology purposes**

# Background analysis in Cr K $\alpha$ HAXPES

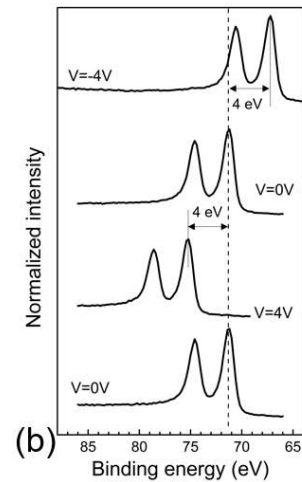
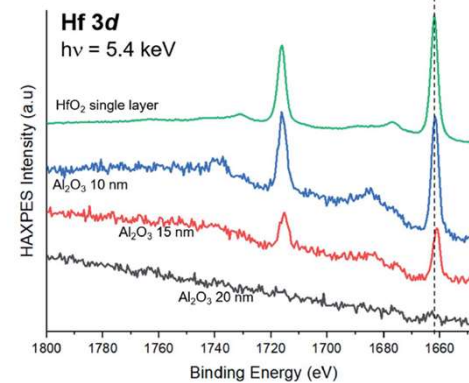
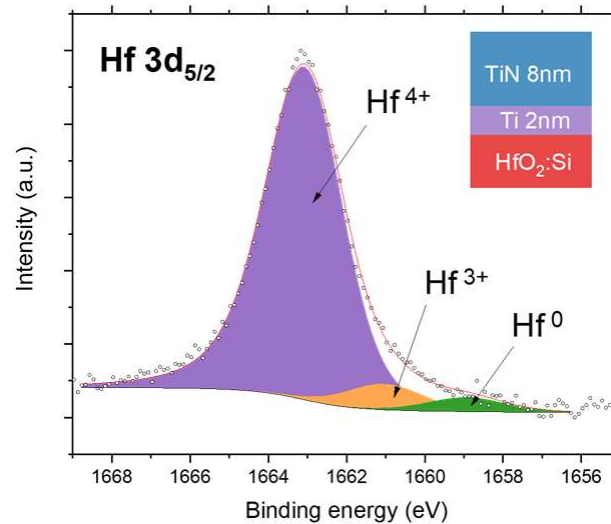
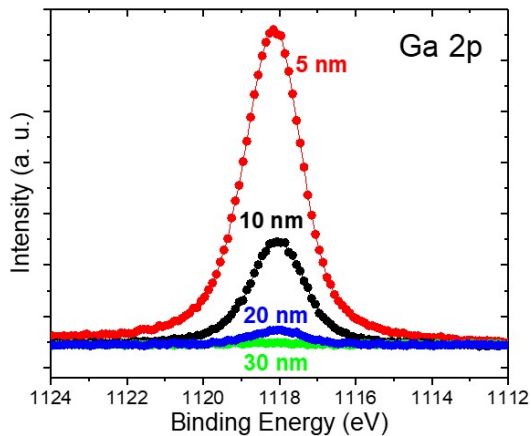


# Operando $K\alpha$ HAXPES of prototypical devices





- **Lab-scale HAXPES with Cr excitation** is promising for device technology
- **Progress in quantification:** updated t-RSFs & extended PERSF databases.
- Extended use of **inelastic background analysis** in lab-HAXPES.
- Novel characterization *operando* approach.



# PlatForm for NanoCharacterisation

*Characterisation of advanced materials and components supporting disruptive innovation*

This unique tool in the world, supported by three CEA Grenoble institutes (CEA-Leti, CEA-Irig and CEA-Liten), aims to develop new characterisation techniques for micro and nanotechnologies, nanomaterials, materials for energy, etc. ; and to carry out the characterizations needed for the advancement of the programs of the CEA and its academic or industrial partners. The expertise of the PFNC covers eight competence centres, including one dedicated to sample preparation, a key step for observations at the nanoscale.

